Extended prediction of QZSS orbit and clock

Helena Leppäkoski, Sakari Rautalin, Xiaolong Zhang, Simo Ali-Löytty, Robert Piché
Tampere University of Technology, Tampere, Finland
Email: {helena.leppakoski, sakari.rautalin, xiaolong.zhang, simo.ali-loytty, robert.piche}@tut.fi

***Abstract*—This paper presents results on the accuracy of the extended (aka autonomous) orbit and clock predictions for the first QZSS satellite in orbit. The purpose of extended prediction is the reduction of the time-to-first-fix of a stand-alone satellite navigation receiver and the improvement of the availability of positioning during weak signal conditions. We describe the models we used to predict satellite orbit and clock and present the prediction accuracies we obtained with our models. With a constant-parameter solar radiation pressure (SRP) model, we obtained orbit prediction accuracies of 8, 25, and 80 m for prediction lengths of 3, 7, and 14 days, respectively. With an SRP model with seasonally varying parameters the accuracies for prediction lengths of 3, 7, and 14 days are 7, 14, and 34 m, respectively. When predicting the QZSS clock for 7 days, the 68% and 95% quantiles of the accumulated prediction errors were 9 and 24 m when using parameters with age of 7 days, 13 and 33 m with age of 14 days, and 22 and 62 m with age of 28 days.**

I. Introduction

This paper presents results on extended prediction of the orbit and clock of the first satellite in orbit of the Quasi-Zenith Satellite System (QZSS) [1]. In satellite-based navigation, extended prediction is used to improve the availability and time-to-first-fix. To estimate its position, the Satellite Navigation System (SNS) receiver needs to know the positions of the navigation satellites and the time offsets of the clocks onboard the satellites with respect to the system time. A SNS receiver operating in stand-alone mode computes these values from the ephemeris and clock parameters that it obtains from the navigation message broadcast by the satellites [2]. However, obtaining the needed parameters from the navigation message takes 30 s in good signal conditions; in weak signal conditions the required time may be much longer. Even if the receiver is able to perform the ranging measurements, the signal strength may drop below the level where decoding the navigation message is possible, which disables the satellite-based positioning. In comparison with an assisted-SNS, the extended prediction also reduces data communications in mobile networks, which is important especially while the receiver is roaming abroad.

Extended satellite orbit and clock prediction (also known as autonomous prediction) provides a means to circumvent these problems by extending the time during which the earlier received ephemeris and clock data is valid. The orbit and clock predictions based on the equations given in interface specifications of the SNS systems are valid only a few hours: e.g., for GPS and QZSS, the fit intervals are typically 4 and 2 hours, respectively [3], [4]. Predictions that are valid for longer periods can be obtained using mathematical and statistical models fitted to Broadcast Ephemeris (BE) data. Commercial services providing extended prediction of GPS and GLONASS ephemerides exist, e.g., [5], [6].

In this paper, we present results on the accuracy of the extended orbit and clock predictions for the first QZSS satellite. To our knowledge, QZSS performance analyses from this perspective have not been published earlier. We use a force model similar to the one described in [7] and the initial kinematic state fitting algorithm described in [8].

To account for the effect of the solar radiation pressure (SRP), we use a two-parameter model for SRP similar to the one presented in [9]. In [10] it was shown that for GPS, the accuracy can be improved by taking into account the seasonal variation of the SRP parameters. We therefore also model the seasonal variation of the SRP parameters and compare the results with the accuracy obtained with the two-parameter model. However, we model the seasonal SRP parameter variation differently from [10] to obtain a better fit to QZSS.

The extended prediction of the offsets of GPS satellite clocks using Kalman Filter (KF) based techniques was presented in [11]. In this paper, we use polynomial fitting for the prediction of QZSS clock. The reason for choosing polynomial fitting instead of KF-based methods is the easy implementation of the algorithm and simple generalization to all satellite systems.

The rest of this article is organized as follows: in Section II we describe the models we use for QZSS orbit and clock prediction. In Section III we describe the processing steps needed for the prediction. The empirical setup and the accuracy results on the QZSS orbit and clock prediction are presented in Section IV and in Section VI we conclude the article.

II. Orbit and clock models

In this section we present the models we use in the extended prediction of the satellite orbit and clock.

A. Extended orbit prediction

In our force model, we consider the four biggest forces acting on a satellite. Thus, the model for the satellite's equation of motion is given by

$$\ddot{\mathbf{r}}_{\text{Sat}} = \mathbf{a}_{\text{Earth}} + \mathbf{a}_{\text{Sun}} + \mathbf{a}_{\text{Moon}} + \mathbf{a}_{\text{SRP}}\,, \tag{1}$$

where $\mathbf{a}_{\text{Earth}}$, $\mathbf{a}_{\text{Sun}}$ and $\mathbf{a}_{\text{Moon}}$ are accelerations caused by the gravitation of the Earth, the Sun and the Moon. The final term $\mathbf{a}_{\text{SRP}}$ is the acceleration caused by SRP. Our force model is largely based on what is described in [12].

2016 International Conference on Localization and GNSS (ICL-GNSS) Barcelona
DOI 10.1109/ICL-GNSS.2016.7533689

For the gravity of the Earth, we use spherical harmonics expansion up to the degree and order 8. The gravity potential of the Earth is calculated as

$$U_{\mathrm{E}} = \frac{GM_{\mathrm{E}}}{r} \sum_{n=0}^{\infty} \sum_{m=0}^{n} \left[\left(\frac{R_{\mathrm{E}}}{r} \right)^n P_{nm}(\sin\phi) \left(C_{nm}\cos(m\lambda) + S_{nm}\sin(m\lambda) \right) \right], \tag{2}$$

where r is the distance of the satellite to the Earth, R_{E} is the Earth's radius, λ is the longitude and ϕ is the latitude. The terms P_{nm} are the associated Legendre polynomials of degree n and order m. The values for the coefficients C_{nm} and S_{nm} are from EGM2008 model [13]. The potential needs to be calculated in ECEF frame and, denoting the transformation matrix from inertial coordinate system to ECEF as R, we may calculate the acceleration caused by Earth in the inertial frame with

$$\mathbf{a}_{\text{Earth}} = \mathrm{R}^{-1} \nabla U_{\mathrm{E}}\,, \tag{3}$$

where ∇ denotes the gradient.

The Sun and the Moon are considered as point masses. The acceleration caused by a celestial body due to gravitation is

$$\mathbf{a}_{\text{cb}} = GM_{\text{cb}} \left(\frac{\mathbf{r}_{\text{cb}} - \mathbf{r}}{||\mathbf{r}_{\text{cb}} - \mathbf{r}||^3} - \frac{\mathbf{r}_{\text{cb}}}{||\mathbf{r}_{\text{cb}}||^3} \right), \tag{4}$$

where M_{cb} is the mass of the body, $\mathbf{r}_{\text{cb}}$ is its position in an Earth-centered inertial frame, and $\mathbf{r}$ is the position of the satellite in the same frame.

For solar radiation pressure, we use a two-parameter empirical model

$$\mathbf{a}_{\text{SRP}} = \nu \big(-\alpha_1 \frac{1}{||\mathbf{r}_{\mathrm{S}}||^3} \mathbf{r}_{\mathrm{S}} + \alpha_2 \mathbf{e}_{\mathrm{y}} \big), \tag{5}$$

where α_1 and α_2 are parameters that we estimate by fitting our force model to the precise orbit data [9]. Vector $\mathbf{r}_{\mathrm{S}}$ points from the satellite to the Sun, i.e., $\mathbf{r}_{\mathrm{S}} = \mathbf{r}_{\text{Sun}} - \mathbf{r}_{\text{Sat}}$, and $\mathbf{e}_{\mathrm{y}}$ is the unit vector to the satellite's y-direction, which is defined as

$$\mathbf{e}_{\mathrm{y}} = \frac{\mathbf{r}_{\text{Sat}} \times \mathbf{r}_{\mathrm{S}}}{||\mathbf{r}_{\text{Sat}} \times \mathbf{r}_{\mathrm{S}}||}\,, \tag{6}$$

where the symbol $\times$ denotes vector product. Parameter $\nu \in [0, 1]$ is a factor that accounts for the Earth's shadow, with $\nu = 1$ when the satellite is not in Earth's shadow and $\nu = 0$ when it is fully in Earth's shadow. We use the conical model for Earth's shadow described in [12].

To take into account the seasonal variation of the SRP parameters, we model them as functions of β, the angle between the vector pointing from the center of the Earth to the Sun and its projection onto the orbital plane of the satellite:

$$\beta = \frac{\pi}{2} - \arccos(\mathbf{e}_{\text{Sun}} \cdot \mathbf{e}_{\mathrm{H}}), \tag{7}$$

where dot $(\cdot)$ denotes scalar product, $\mathbf{e}_{\text{Sun}}$ is unit vector in the direction from the center of the Earth to the center of the Sun and $\mathbf{e}_{\mathrm{H}}$ is the unit vector normal to the orbital plane of the satellite, obtained as

$$\mathbf{e}_{\mathrm{H}} = \frac{\mathbf{r}_{\text{Sat}} \times \mathbf{v}_{\text{Sat}}}{||\mathbf{r}_{\text{Sat}} \times \mathbf{v}_{\text{Sat}}||}\,. \tag{8}$$

We compute the SRP parameters α_1 and α_2 as polynomials of functions of β. As α_2 seems to perform a monotonic change during a half cycle of β, also the direction of β change is needed for the model. We use the following functions of β and its derivative $\dot{\beta}$:

$$x_1 = 2 \left(\frac{|\beta|}{\beta_{\text{max}}} - 1 \right) \text{sign}(\dot{\beta})\,, \tag{9}$$

$$x_2 = 2 \left(\arccos(x_1) - \frac{\pi}{2} \right), \tag{10}$$

where β_{max} is the maximum value of β in its cycle in radians, approximately $64°$ (≈ 1.1 rad). The polynomials for computing the SRP parameters are

$$\alpha_1(x_1) = b_1 x_1 + b_0\,, \tag{11}$$

$$\alpha_2(x_2) = c_3 x_2^3 + c_1 x_2 + c_0\,, \tag{12}$$

where b_1, b_0, c_3, c_1, and c_0 are obtained by fitting the polynomial terms of x_1 and x_2 to weekly estimates of α_1 and α_2 that are obtained using Precise Ephemeris (PE) data of the QZSS satellite [14].

B. Broadcast clock model and clock prediction

The model for the clocks of QZSS is similar to the model for GPS clocks. The clock bias τ at time t is modelled as

$$\tau(t) = a_0 + a_1(t - t_{\text{toe}}) + a_2(t - t_{\text{toe}})^2, \tag{13}$$

where t_{toe} is the time of ephemeris, parameter a_0 is current clock offset, a_1 is the clock drift and a_2 is the clock drift rate. These parameters are given in the BE data [4]. In principle, they could be used to directly predict the clock offset in the future. They are, however, quite inaccurate for long-term predictions. Therefore, these parameters have to be estimated in a different way.

We noticed that the broadcast value for a_2 is a multiple of $2.7756 \cdot 10^{-17}$. For the time intervals for which BEs are normally used, this does not cause problems, but when our predictions span days or even weeks, this parameter causes a very large error: in one-week prediction, the difference is $1.0 \cdot 10^{-5}$ s, which corresponds to 3 km in position error. Therefore, in testing and in method comparison, we use $a_2 = 0$ as the BE value. This is also mentioned in the QZSS interface document as the correct procedure when there is ephemeris data but not almanac data for the clock [4].

We use a polynomial fitting model for clocks, i.e., we fit second order polynomial to the data using least-squares algorithm and use these parameters as our estimates. This approach has been used for GPS for example in [15] to predict the clock offset.

We obtain our long term estimates of a_1 and a_2 by fitting the polynomial terms to a series of a_0 values obtained from BEs.

For a_2, we use one-week fitting window and for a_1 we use one-day fitting window. First we fit quadratic model and then use the estimated value of a_2 to subtract the quadratic trend from the data. Then a linear model is used when fitting a_1. This is done due to different lengths of the fitting windows. For a_0 we simply use the value supplied by the BE at the reference epoch of our prediction model.

In our study (Section IV-C) we also look into how the age of the parameters affects the results. This determines how often the parameters a_1 and a_2 have to be updated in the device.

III. Procedures for extended orbit prediction

For the orbit prediction, the SRP parameters, antenna correction, the initial position and velocity of the satellite, and the Earth orientation parameters need to be known.

A. Offline estimation of parameters

As the estimation of the SRP parameters and antenna correction require large amounts of data and computation power, these parameters need to be estimated offline on the server.

We estimate the SRP parameters of (5) offline by fitting the force model (1)–(5) to the PE data. For constant two-parameter model, we compute the estimates of α_1 and α_2 for several one-week intervals and then take the medians of the weekly estimates. For example, using the PE data of the year 2013 we obtain $\alpha_1 = 2.263$ and $\alpha_2 = -0.460 \times 10^{-9}$. For seasonal SRP model, we compute the β angles with (7) and use equations (9)–(12) to fit the polynomial coefficients to the weekly estimates of α_1 and α_2.

To start the prediction using (1)–(5), the position of the mass center of the satellite should be known. However, the position obtained from BE is the position of the antenna phase center of the satellite. In order to use BE to initialize the prediction, antenna correction, i.e., the difference between the satellite's center of mass and antenna phase center need to be known. As the PE reports the coordinates of the mass center of the satellite, the antenna correction can be computed by comparing the satellite coordinates from BE and PE. Although the values of the correction are also available in [16], we use in our study the correction obtained using BE and PE. As the antenna correction is constant, we precompute it. To mitigate the effect of inaccuracy of BE, we sample the BE and PE data from one year in two hour intervals, compute the coordinate differences, and use the median of these as the correction.

B. Initialization

Position and velocity from the BE are not directly suitable to be used as an initial state for the extended prediction. The initial position and velocity must be calculated by adjusting the BE data to the dynamic model used in the prediction.

We use extended Kalman filter to get an estimate for the initial state. The BE positions and velocities of the satellite for the interval from $t_{\text{toe}} - 1.5\,\text{h}$ to $t_{\text{toe}} + 1.5\,\text{h}$, sampled in intervals of 15 minutes, are filtered to get an estimate for the initial state. During this phase, we also estimate the Earth Orientation Parameters (EOP). The details of the method can be found in [8].

TABLE I
Availability of prediction during weeks 1749-1868

Data problem	% of total time
BE missing	0.60
BE health > 1	0.79
PE missing	1.44
Zero coordinates in PE	0.87
Outage issued in NAQU	1.34
Initialization impossible (BE, NAQU)	1.86
Initialization unreliable (BE, NAQU, PE)	3.82
Prediction unavailable or unreliable	**% of total time**
For intervals of 3 days	12.7
For intervals of 7 days	23.7
For intervals of 14 days	40.5

C. Orbit prediction

The estimated initial state is used as an initial condition for equation (1). We integrate the equation numerically to estimate the position and velocity of the satellite at a later time.

We use 8th order Gauss-Jackson integrator with 15-minute time step to evaluate the position and velocity of the satellite. The predicted states are stored to the device. These predicted orbit values can be used directly, or Keplerian parameters can be fitted [17] to provide orbit information in BE format.

IV. Results

In this section we present our results on prediction of QZSS orbit and clock. Our analyses are based on the data that is available on the download site of QZSS [14], where both the BE and PE files are available. Notice Advisory to QZSS Users (NAQU) messages, i.e., QZSS equivalents of the NANU (Notice Advisory to NAVSTAR Users) messages, are also available on the website.

A. Observations on QZSS ephemeris data

With QZSS, a new BE is issued at 15 min intervals, i.e., *Issue of Data Ephemeris* (IODE) and *Time of Ephemeris* TOE update also at this interval. This is different from e.g. GPS that issues the new BE at 2 h intervals. The fit interval of QZSS BE is 2 h, which is shorter than the 4 h fit interval of GPS.

We studied all the QZSS BEs between GPS weeks 1800 and 1865 and found that the health value was always at least 1, i.e., the health did never get the value 0. We also found that within the studied interval, the health rises from 1 at the times when QZSS outages are issued in NAQUs. We are aware that according to the Interface Specification [4], only health value 0 denotes a healthy satellite. However, as the health never got that value, for the present we interpret the value 1 as the normal state.

We also found outages of QZSS BEs or PEs, i.e., some `rinex` or `sp3` files are missing in the server [14]; in some cases `sp3` file exist but reports zeros as the satellite coordinates. Typically ephemeris files or data were missing at the times when QZSS outages are issued in NAQU messages.

As the initialization of the prediction is impossible if BE is missing, and the prediction performance cannot be assessed if the PE data for the reference orbit is missing, we excluded the intervals of missing ephemeris data from our orbit prediction analyses.

The tests also indicated that even if none of these exceptions (`health` > 1, outage issued in NAQU, or BE or PE missing) affected the initialization epoch nor the end of the prediction but happened during the prediction interval, quite often the orbit prediction error was unusually high at the end of the prediction. In these cases, the errors at the end of the two weeks prediction interval can be even hundreds of kilometers. This suggests that during these prediction intervals, the orbit of the satellite changes more than usually, and therefore the BE of the initialization epoch does not provide sufficient information for longer prediction intervals. Therefore, from the performance comparisons we have excluded all the predictions where any of these exceptions are present either in the initialization epoch, during the prediction interval, or at its end. The statistics of the availability of orbit prediction during weeks 1749-1868 are given in Table I. We point out that there is a difference between the occasions when the initialization of the prediction is impossible and when it is unreliable. A real-time application can judge the possibility of initialization by checking the BE and NAQU but the assessment of the reliability of the initialization is possible only in post-processing as the PE is not available in real time.

B. Orbit prediction results

Satellite orbital error is often expressed with error components in the radial (from Earth to satellite), tangential (satellite velocity direction), and normal (perpendicular to the other two) directions. These different components contribute to the positioning error in different ways. The effects of the Radial, Tangential, and Normal (RTN) components can be combined to Signal In Space Range Error (SISRE), which includes also the effect of the satellite clock error. SNS receivers at different locations on the Earth experience different SISRE as the SISRE depends on the satellite-user geometry. According to [18], the global-average SISRE for the orbit-only case, neglecting the clock errors, can be written for the QZSS satellite as

$$\sigma_{\mathrm{SISRE}} = \sqrt{(0.99 \cdot \sigma_{\Delta R})^2 + \frac{1}{126}(\sigma_{\Delta T}^2 + \sigma_{\Delta N}^2)}\,, \qquad (14)$$

where $\sigma_{\Delta R}^2$, $\sigma_{\Delta T}^2$ and $\sigma_{\Delta N}^2$ represent the mean-square errors of radial, tangential and normal direction errors, respectively. Other SNS systems have their own formulae, which are quite similar, only with differences in the coefficients [18].

In this paper, we assess the performance of the orbit prediction using (14) and evaluate σ_{SISRE} by comparing the predicted orbit with the PE.

1) Performance with two-parameter SRP model: To evaluate the performance of the orbit prediction, we computed the predictions for 119 GPS weeks, from the week 1749 to 1867. The prediction tests were started at 1 h intervals, the predictions were made in 15 min intervals, and the time span of each test was 14 days.

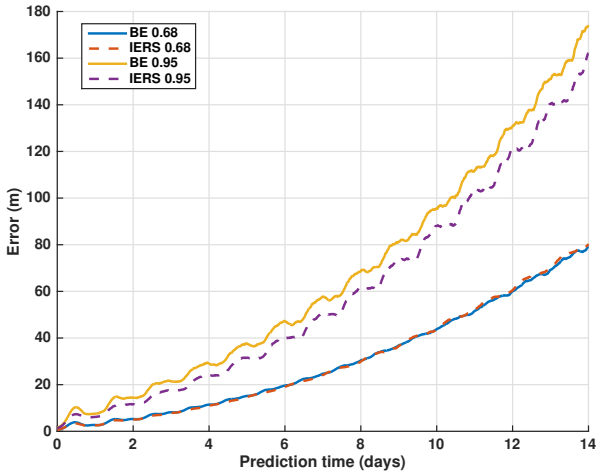

Fig. 1. 68% and 95% quantiles of the prediction errors: orbit only SISRE as functions of prediction time: EOP estimated from BE and precise EOP from IERS.

Fig. 1 shows the 68% and 95% quantiles of the orbit only SISRE errors as a function of the prediction length. In the figure we show results of predictions where the EOP is obtained from the initial state estimation based on BE compared to results obtained using the precise EOP from IERS [19]. It can be seen that while the accuracy difference between the EOPs is small in the 68% quantile, the precise EOP decreases the amount of large errors. The 68% quantiles for prediction lengths of 3, 7, and 14 days are about 8, 25, and 80 m.

In Fig. 2, the SISREs from 3 days long predictions are shown as the functions of the ends of the prediction intervals. The figure shows also the β angle. In the error, higher peaks repeat in 26 weeks, around the times when β changes its sign.

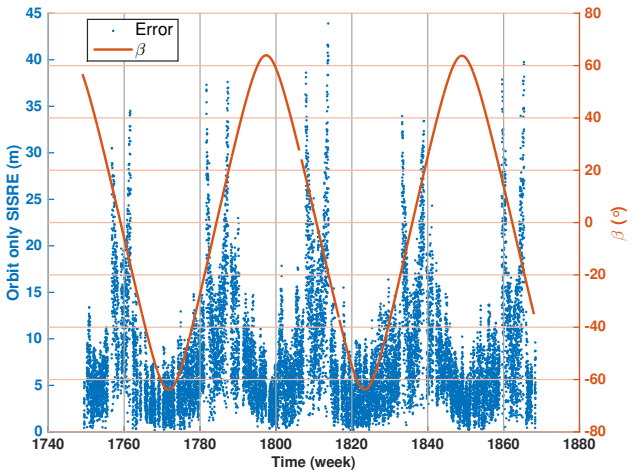

Fig. 2. Orbit only SISRE at the end of 3 days' prediction and β angle as functions of time. (Here β is shown in degrees but in computations it is expressed in radians.)

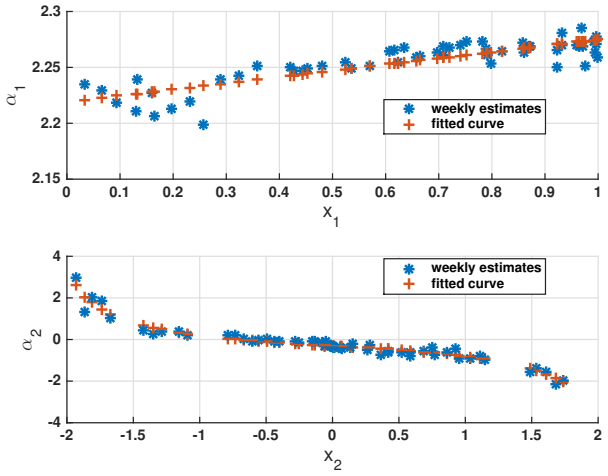

Fig. 3. SRP parameters α_1 and α_2 of weeks 1749 – 1824 as functions of x_1 and x_2: weekly estimates and polynomials fitted to them.

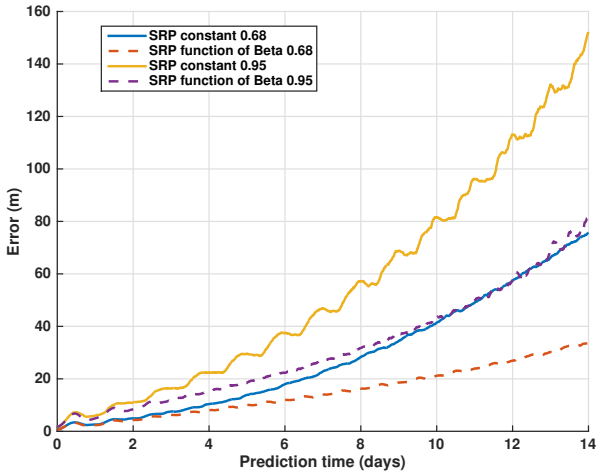

Fig. 5. 68% and 95% quantiles of the prediction errors: orbit only SISRE as functions of prediction time: constant SPR parameters vs SRP parameters as functions of Beta angle.

2) Performance with seasonal SRP model: By inspecting the weekly estimates of the SRP parameters we found that there is a repeating pattern in their variation and the period of the variation turned out to be the half cycle of β. Fig. 3 shows the weekly estimates of SRP parameters as functions of x_1 and x_2 which are obtained as functions of β and $\dot{\beta}$. It shows also the estimated α_1 and α_2 values that are computed using polynomials (11) and (12) fitted to the weekly estimates.

Fig. 4 shows the weekly estimates of SRP parameters and the values of polynomials (11) and (12) as a function of time for weeks 1749 – 1868. The polynomials are fitted to weekly estimates of weeks 1749 – 1824 (64% of data); the weekly estimates of weeks 1825 – 1868 (36% of data) demonstrate the accuracy of the fitted polynomials.

The orbit prediction accuracies obtained using SRP model with constant parameters and with seasonal model for weeks 1825 – 1876 are shown in Fig. 5. The parameters for the seasonal model were obtained from the data of weeks 1749 – 1824. The results show significant improvement by using seasonal SRP model: in 68% quantile, the prediction error at 14 days decreases 55% from 76 m to 34 m. In 95% quantile, the error at 14 days decreases 45% from 151 m to 83 m. For the same data, Fig. 6 shows the RTN components of the errors for 7 days prediction. It can be seen that the seasonal SRP model reduces radial and tangential error components but the effect is negligible on normal component.

The reason for smaller improvement in 68% quantile compared to 95% quantile can be seen in Fig. 7, where orbit only SISREs for prediction lengths 3 and 14 days are shown as functions of the end times of prediction intervals. In general, the seasonal SRP parameters improve prediction. However,

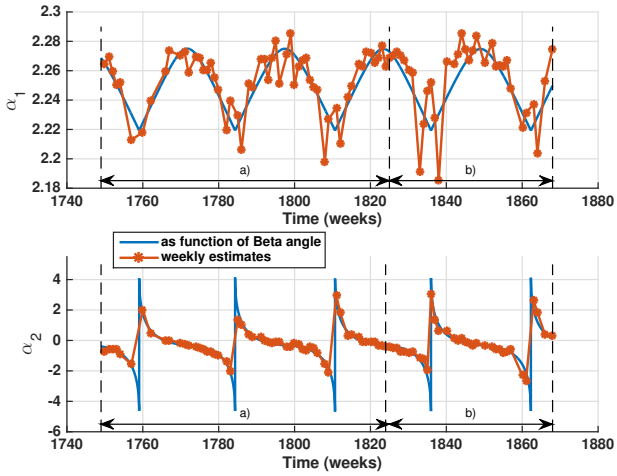

Fig. 4. SRP parameters α_1 and α_2 as functions of time. The data used for fitting the polynomial coefficients is from the interval a). In the interval b) the SRP parameters are estimated using the polynomial fit from the interval a).

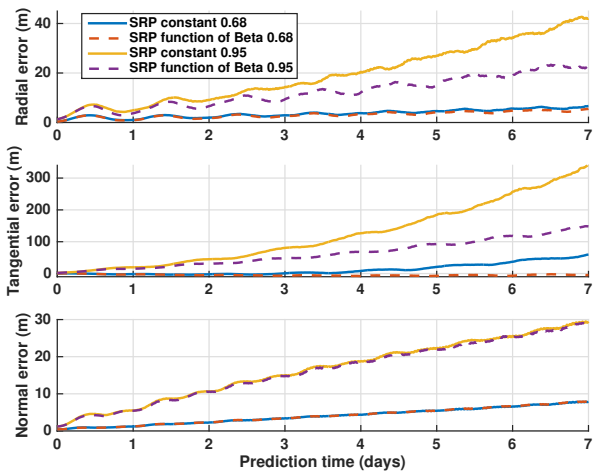

Fig. 6. 68% and 95% quantiles of the prediction errors in Radial, Tangential and Normal directions as functions of prediction time: constant SPR parameters vs SRP parameters as functions of Beta angle.

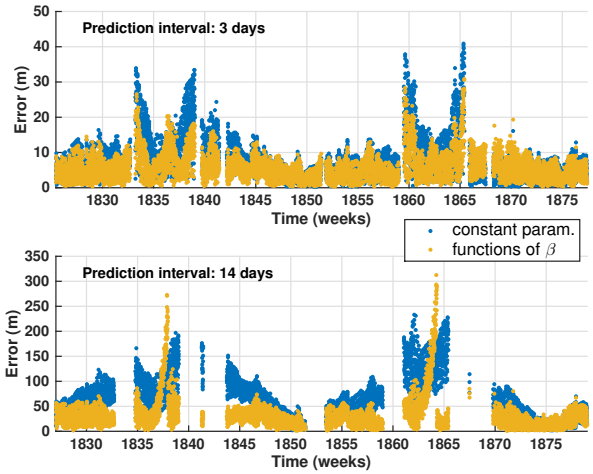

Fig. 7. Orbit only SISRE at the end of the prediction interval obtained using constant SRP parameters and seasonal parameters as functions of β.

during weeks 1836 and 1862 the prediction using seasonal SRP parameters produce error peaks that are higher than the errors obtained with constant SRP parameters. In the 14 days prediction the difference is more visible. During these weeks β angle crosses zero; close to the zero crossings of β, the constant SRP parameter model produces better predictions than the seasonal model.

The data gaps visible in Figs. 2 and 7 are due to the data problems, listed in Table I, and their effect on the availability of reliable prediction; the results that were considered unreliable due to the data problems are not shown in the figures.

C. Clock prediction results

Our testing period was from start of 2014 until June 2015. We used one ephemeris every hour and compared the prediction accuracy with different aged parameters to the prediction accuracy of the broadcast parameters.

In Fig. 8 and Fig. 9 we have 68% and 95% error quantiles for different methods and fit ages of the parameters. Error is transformed to meters by multiplying with the speed of light. We see that with fitted coefficients, parameters that are weeks or even months old, we get much better results than using only BE data.

V. Discussion

The results presented in Section IV indicate that the extended prediction of QZSS orbit and clock can be used to improve the availability and time-to-first-fix in stand-alone GNSS receivers that have challenges to obtain the BE from the navigation message. However, this always happens at the expense of the positioning accuracy, as even the accurate prediction models include errors. With our models, the 68% and 95% quantiles of the QZSS orbit-only SISRE are 10 m and 19 m in 5 days prediction, respectively. The corresponding 68% quantiles for RTN errors are 15, 93, and 22 m and 95% quantiles are 27, 184, 22 m. For the QZSS clock errors using parameters of age 0 days, the error quantiles after 5 days prediction are 4 m and 14 m.

Similar orbit prediction models but without taking into account the seasonal SRP variation were used for GPS and GLONASS prediction in [9]. For 5 days prediction of GPS, they obtained 95% quantiles 3.4, 72.3, and 11.1 m for orbital RTN errors. For GLONASS, the corresponding results were 4.0, 85.4, and 15.0 m in RTN directions. Comparing the performance figures of QZSS with these, we conclude that the QZSS orbit seems to be more difficult to predict.

VI. Conclusions

In this paper we present results on the accuracy of the extended orbit and clock predictions for the first QZSS satellite on orbit. To our knowledge, these are the first published results regarding the extended orbit and clock prediction of a QZSS satellite. We present results on orbit prediction using both the constant SRP parameters and seasonal SRP parameters that change as a function of beta angle. Our results show that when the BE and NAQU data of QZSS are reliable, the BE

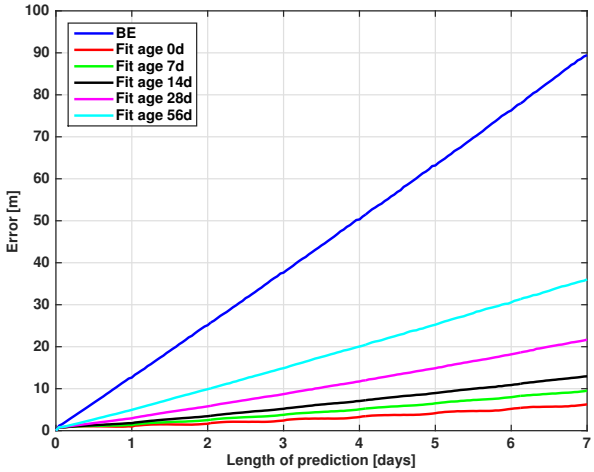

Fig. 8. Clock prediction: 68% quantile of the prediction errors.

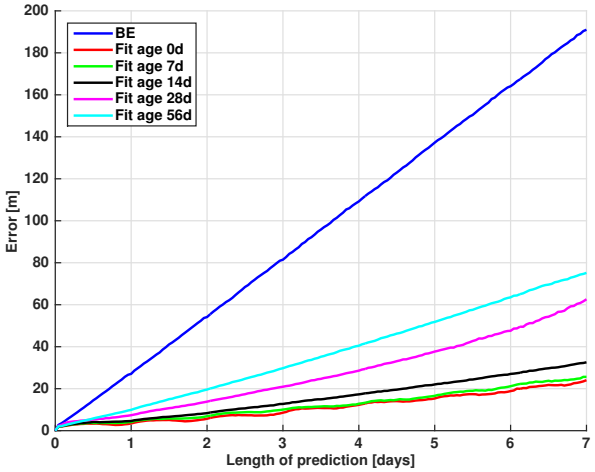

Fig. 9. Clock prediction: 95% quantile of the prediction errors.

accuracy allows the extended orbit and clock prediction on the receiver by using our models. However, more analysis is needed to confirm when the QZSS data is reliable to be used in prediction. Further research is also needed to explain the higher errors at the times when solar elevation angle β is near zero and to identify the most sensitive parameters and the major limitations of the prediction models.

ACKNOWLEDGMENT

The authors would like to thank HERE Global B.V. for the financial support, guidance and collaboration during this research.

REFERENCES

[1] Quasi-Zenith Satellite-1 "MICHIBIKI". [Online]. Available: http://global.jaxa.jp/projects/sat/qzss/index.html

[2] P. Misra and P. Enge, *Global Positioning System: Signals, Measurements, and Performance*, 2nd ed. Ganga-Jamuna Press, 2006.

[3] Global Positioning Systems Directorate, Systems Engineering & Integration, "Interface specification IS-GPS-200," Tech. Rep., 2013. [Online]. Available: http://www.gps.gov/technical/icwg/IS-GPS-200H.pdf

[4] "Interface specification for QZSS (IS-QZSS) v 1.6," Japan Aerospace Exploration Agency, Tech. Rep., 2014. [Online]. Available: http://qz-vision.jaxa.jp/USE/is-qzss/DOCS/IS-QZSS_16_E.pdf

[5] C.-T. Weng, Y.-C. Chien, C.-L. Fu, W.-G. Yau, and Y. Tsai, "A broadcast ephemeris extension method for standalone mobile apparatus," in *the 22nd International Technical Meeting of The Satellite Division of the Institute of Navigation (ION GNSS 2009)*, Savannah, GA, USA, 2009, pp. 2108–2114.

[6] Baseband Technologies Inc. 28 day extended ephemeris. [Online]. Available: http://basebandtech.com/28-day-extended-ephemeris/

[7] M. Seppänen, J. Ala-Luhtala, R. Piché, S. Martikainen, and S. Ali-Löytty, "Autonomous prediction of GPS and GLONASS satellite orbits," *NAVIGATION*, vol. 59, no. 2, pp. 119–134, 2012.

[8] J. Ala-Luhtala, M. Seppänen, S. Ali-Löytty, R. Piché, and H. Nurminen, "Estimation of initial state and model parameters for autonomous GNSS orbit prediction estimation of initial state and model parameters for autonomous GNSS orbit prediction," in *International Global Navigation Satellite Systems Society Symposium 2013 (IGNSS2013)*, Gold Coast, Queensland, Australia, July 2013.

[9] J. Ala-Luhtala, M. Seppänen, and R. Piché, "An empirical solar radiation pressure model for autonomous GNSS orbit prediction," in *Proceedings of PLANS 2012 IEEE/ION Position Location and Navigation Symposium*, April 2012, pp. 568–575.

[10] A. Pukkila, J. Ala-Luhtala, R. Piché, and S. Ali-Löytty, "GNSS orbit prediction with enhanced force model," in *Localization and GNSS (ICL-GNSS), 2015 International Conference on*. Gothenburg, Sweden: IEEE, 2015, pp. 1–6.

[11] S. Martikainen, R. Piché, and S. Ali-Löytty, "Outlier-robust estimation of GPS satellite clock offsets," in *Localization and GNSS (ICL-GNSS), 2012 International Conference on*, Starnberg, Germany, June 2012, pp. 1–5.

[12] O. Montenbruck and E. Gill, *Satellite Orbits: Models, Methods and Applications*, 3rd ed. Springer, 2005.

[13] NGA. EGM2008 model coeffcients. [Online]. Available: http://earth-info.nga.mil/GandG/wgs84/gravitymod/egm2008/first_release.html

[14] QZ-vision. QZSS+GPS data download. [Online]. Available: http://qz-vision.jaxa.jp/USE/en

[15] Z. Y. Zheng Zuoya, Chen Yongqi, "A study on the prediction of gps satellite clock bias with igs ultra-rapid products – preliminary results," 2007.

[16] O. Montenbruck, R. Schmid, F. Mercier, P. Steigenberger, C. Noll, R. Fatkulin, S. Kogure, and A. Ganeshan, "Gnss satellite geometry and attitude models." *Advances in Space Research*, vol. 56, no. 6, pp. 1015–1029, 2015.

[17] H. Kosola, S. Ali-Löytty, and R. Piché, "Converting GNSS satellite orbit segments to GPS-compatible format," in *Ubiquitous Positioning Indoor Navigation and Location Based Service (UPINLBS2012)*, October 2012, pp. 1–5.

[18] O. Montenbruck, P. Steigenberger, and A. Hauschild, "Broadcast versus precise ephemerides: a multi-GNSS perspective." *GPS Solutions*, vol. 19, no. 2, pp. 321–333, 2015.

[19] International Earth Rotation and Reference Systems Service (IERS). Earth orientation data. [Online]. Available: http://www.iers.org/IERS/EN/DataProducts/EarthOrientationData/eop.html